

## Research article

# Oxytocin receptor enhances adipocyte browning and energy metabolism in mice

Xinyue Bao<sup>a,1</sup>, Mingjun San<sup>b,1</sup>, Shuilian Wang<sup>a</sup>, Yanli Zhuo<sup>c</sup>, Ziying Liu<sup>a</sup>, Yaowu Zheng<sup>b,\*</sup>, Dan Li<sup>a,\*\*</sup>

<sup>a</sup> Department of Basic Medicine, Shenyang Medical College, Shenyang, Liaoning, 110034, China

<sup>b</sup> Transgenic Research Center, Northeast Normal University, Changchun, Jilin, 130024, China

<sup>c</sup> Room of drug inspection (II), Shenyang Institute for Food and Drug Control, Shenyang, Liaoning, 110000, China

## ARTICLE INFO

## Keywords:

OXTR  
White adipose tissue (WAT)  
Brown adipose tissue (BAT)  
Energy metabolism

## ABSTRACT

Obesity is characterized by abnormal adipose tissue development and disrupted energy metabolism, involving multiple factors. Oxytocin receptor (OXTR) influences social behaviors, mammary gland development and reproduction. In this study, a transgenic mouse model with universal OXTR overexpression under the  $\beta$ -actin promoter ( $^{++}Oxtr$ ) was employed. Both  $^{++}Oxtr$  males and females exhibited a lean phenotype with reduced fat accumulation, despite unchanged food consumption. OXTR overexpression enhanced energy expenditure, adaptive thermogenesis and glucose tolerance. Morphologically, OXTR overexpression induced adipose tissue browning, marked by increased cell density and smaller adipocytes. Gene expression analysis revealed elevated levels of Brown Adipose Tissue (BAT) markers, fatty acid transport proteins and glucose transporters in adipose tissues. High OXTR ameliorated high-fat diet (HFD)-induced obesity with improvement of metabolic parameters. Mechanistically, OXTR overexpression led to an activation of PPAR signaling, increased energy expenditure, reduced fat deposition and promoted weight loss. These findings identify OXTR as a critical regulator of energy metabolism and thermogenesis. The ability of OXTR to enhance adaptive thermogenesis and energy metabolism suggests it may serve as a novel therapeutic target for metabolic disorders.

## 1. Introduction

Obesity, a pathological accumulation of body fat, is a global health concern linked to cardiovascular disease, diabetes, infertility and several cancers [1]. Adipose tissue, commonly referred to as 'fat', plays essential roles in regulating various physiological processes, including energy metabolism, food intake, thermogenesis and insulin responses. It is broadly classified as two types, white adipose tissue (WAT) and brown adipose tissue (BAT). WAT, characterized by sparse mitochondria and large lipid droplets, specializes in energy storage and adipokine secretion (e.g., leptin). Subcutaneous WAT (sWAT) or gonadal WAT (gWAT) represent its primary deposits. In contrast, interscapular BAT is distinguished by high mitochondria density and Uncoupling Protein 1 (UCP1), which can exert thermogenesis [2]. Adipose tissue plasticity enables reversible transformation between WAT and BAT. WAT browning can offer protection against weight gain and metabolic disorders by

elevating energy expenditure, thermogenesis and insulin sensitivity [3, 4]. Identifying regulators of WAT browning and energy metabolism is crucial for developing obesity therapies.

Oxytocin Receptor (OXTR), a G-protein coupled receptor, is involved in thermogenesis. OXTR is widely expressed in mammalian tissues, including the brain, reproductive organs, mammary gland, and bone [5]. Its ligand, oxytocin (OXT), is synthesized in the neurons of the paraventricular nucleus (PVN) and the supraoptic nucleus of the hypothalamus and secreted by the posterior lobe [6]. OXTR, in response to OXT binding, processes and transfers signals into the cytoplasm to modulate the downstream events. OXT/OXTR system is implicated in parturition, milk ejection, mammary gland development, bone formation, social behaviors, and cancer progression [7–9]. In mice, hypothalamic OXT-producing neurons in the PVN connect to pancreatic  $\beta$ -cells via sympathetic nerves, ultimately affecting insulin release [10]. Cold exposure upregulates OXT and OXTR expression in BAT and brain [11].

\* Corresponding author.

\*\* Corresponding author.

E-mail addresses: [zhengyw442@nenu.edu.cn](mailto:zhengyw442@nenu.edu.cn) (Y. Zheng), [lidan0519@symc.edu.cn](mailto:lidan0519@symc.edu.cn) (D. Li).

<sup>1</sup> These authors have contributed equally to this work.

Both *Oxtr*-knockout mice (*Oxtr*<sup>-/-</sup>) and *Oxt*-knockout (*Oxt*<sup>-/-</sup>) exhibit impaired cold-induced thermogenesis, diabetes, and late-onset of obesity [12–14], while exogenous OXT can promote thermogenesis and mitigates metabolic dysfunctions [15,16]. These evidences indicate the significant role of OXT system in energy metabolism. Here, we investigated the OXTR's effects in energy metabolism and adipose development using the <sup>++</sup>*Oxtr* mouse model.

## 2. Methods

### 2.1. Animals

Shenyang Medical College Ethics Committee approved all animal research and protocols (SYXY2023061001). The  $\beta$ -actin-*Oxtr* (<sup>++</sup>*Oxtr*) model was generated as previously described in prior studies (Accession RRID: MGI\_6314370) [8,9]. Age-matched WT littermates of the same sex served as controls. All animals (C57/BL6J background) had unlimited access to water and food, and were kept in a pathogen-free environment (21 ± 1 °C, 50 ± 20 % humidity, 12-h dark/light cycle). During twice-weekly monitoring, the signs of lethargy or persistent recumbency served as humane endpoints. Mice were anesthetized intraperitoneally with 1 % pentobarbital sodium (10 mg/kg) prior to euthanasia.

### 2.2. Genotyping

The GNTK buffer [17] (0.01 % gelatin, pH 8.5 10 mM Tris-HCl, 1M MgCl, 250 mM KCl, 0.45 % Tween-20, 0.45 % Nonidet P-40, and 100 mg/mL proteinase K) was used to digest the tail tips overnight at 55 °C. The lysates were boiled for 15 min as DNA templates. PCR were set as follows: initiation 2 min at 94 °C, succeeded by 30 cycles consisting of 30 s at 94 °C, 30 s at 57 °C, and finally 1 min at 72 °C. A final extension was at 72 °C for 10 min. The primers, designed within the *rb\_glob\_PA\_terminator* of the pCAGGS vector, were as follows: AATGCCCTGG-CTCACAAATAC(forward); GGGACAGCTATGACTGGGAGTAG (reverse). <sup>++</sup>*Oxtr* mice yielded a 456bp band, no band in WT mice.

### 2.3. Real-time PCR

Mouse tissues were treated with TRIzol (Takara) for total RNA extraction. 1ug total RNA was reversely transcribed using the Takara's PrimeScript™ RT Reagent kit following the instructions. Real-time PCR (RT-PCR) was performed with ChamQ Universal SYBR qPCR Master Mix from Vazyme. Relative gene expression was calculated using the 2<sup>- $\Delta\Delta$ CT</sup> method, and normalized to 18S ribosomal RNA. Primer sequences can be referenced in [Supplementary Table S1](#).

### 2.4. Food intake and body weight measurement

Body weights and food intake were assessed weekly, with 3–4 mice per cage. A total of 100g of mouse pellets was provided weekly. Food efficiency was calculated as the percentage of increased weight in relation to food intake.

The measurement of serum triglyceride, cholesterol, oxytocin and insulin.

Post-anesthesia, blood was obtained from the orbital venous to sit at 25 °C for 30 min. The samples underwent centrifugation at 3000 rpm for 15 min to separate the serum layer. Cholesterol and triglyceride levels were determined utilizing Hui Li assay kits (Changchun, China). Oxytocin ELISA kit (Enzo, USA) has the sensitivity of 15 pg/mL. Insulin was measured by mouse insulin ELISA (Mercodia).

### 2.5. Histology analysis and immunohistochemistry

For histological examination, fixed and embedded adipose tissues were cut into 5  $\mu$ m sections. These slides were stained with hematoxylin and eosin [18]. For immunohistochemistry [19], an antigen heat

retrieval was conducted using pH 8.0 of EDTA buffer for 15 min. Slides were incubated overnight at 4 °C with the primary antibodies (1:500, Rabbit anti-OXTR, Abcam: ab181077), followed by secondary antibodies (HRP-conjugated anti-rabbit IgG, CST:8114P) for 30 min at 25 °C. Subsequently, the peroxidase signal was visualized as brown using DAB (CST). Nuclei were counterstained with hematoxylin.

### 2.6. Glucose and insulin tolerance test

For Intraperitoneal Glucose Tolerance Test (IPGTT), 11-week-old mice were given libitum access to water and fasted for 16 h. After intraperitoneal administration of 2 g/kg glucose, tail blood glucose was measured using a glucometer (Omron, China) at 0, 15, 30, 45, 60, 75, 90, 105 and 120 min.

For Intraperitoneal Insulin Tolerance Test (IPITT), 11-week-old mice were given libitum access to water and fasted for 4 h. Intraperitoneal administration of 0.75 U/kg insulin was performed, and tail blood glucose was recorded at 0, 15, 30, 45, 60, 75, 90, 105, and 120 min.

### 2.7. The measurement of body temperature and oxygen consumption

Core body temperature was measured rectally with a probe-equipped electronic thermometer (Omron) after 4-h cold exposure (4 °C). Oxygen consumption was assessed using a respirometer with CO<sub>2</sub> absorption in alkaline solution.

### 2.8. RNA sequencing and analysis

WT and <sup>++</sup>*Oxtr* gWAT were sequenced via an Illumina Hiseq 2500. Low-quality reads were trimmed and filtered out [20]. The threshold of Q-value <0.05 and |log<sub>2</sub> (fold change)| >1 was established to identify differentially expressed genes (DEGs) using Cuffdiff software 2.0.0 [21]. Gene ontology (GO) analysis was carried out via a GOrilla tool. P-values were adjusted according to False Discovery Rate (FDR) [22]. Significantly enriched GO terms were set as q value < 0.05. Heatmaps were generated with OmicShare tools2. GeneVenn's tool online was employed. No batch effects were involved due to the same batch for uniform sequencing conditions. Key DEGs were validated using independent methods RT-PCR.

### 2.9. Statistical analysis

All statistical analysis were conducted using Prism 9 (GraphPad). Quantitative measurements were employed by ImageJ. No statistical methods were used to predetermine sample size or conduct power analysis. Mean differences (MD) with 95 % confidence intervals (95 % CI) were calculated. For all experiments except RNA-seq, each experiment was conducted independently at least three times, yielding consistent results. Age-matched WT littermates of the same sex served as the control group. All data were included in the analysis with no exclusions. The specific sample sizes (n numbers) were provided in figure legends. The data presented were indicated as Means ± SD. Statistically significant levels were obtained using unpaired two-tailed Student's t-tests for comparisons of WT and <sup>++</sup>*Oxtr* groups. \*\*\*P < 0.001, \*\*P < 0.01, \*P < 0.05.

## 3. Results

### 3.1. *Oxtr* overexpression induces loss of body fat and body weight

To explore the role of OXTR in metabolism, transgenic mice with universal overexpression of OXTR under the  $\beta$ -actin promoter (<sup>++</sup>*Oxtr*) were employed [8,9]. OXTR overexpression was confirmed in gWAT, sWAT and BAT (Figs. S1A and B). However, no difference was found in serum oxytocin between WT and <sup>++</sup>*Oxtr* mice (Fig. S1C). On a regular chow diet, <sup>++</sup>*Oxtr* mice exhibited a leaner phenotype than their WT

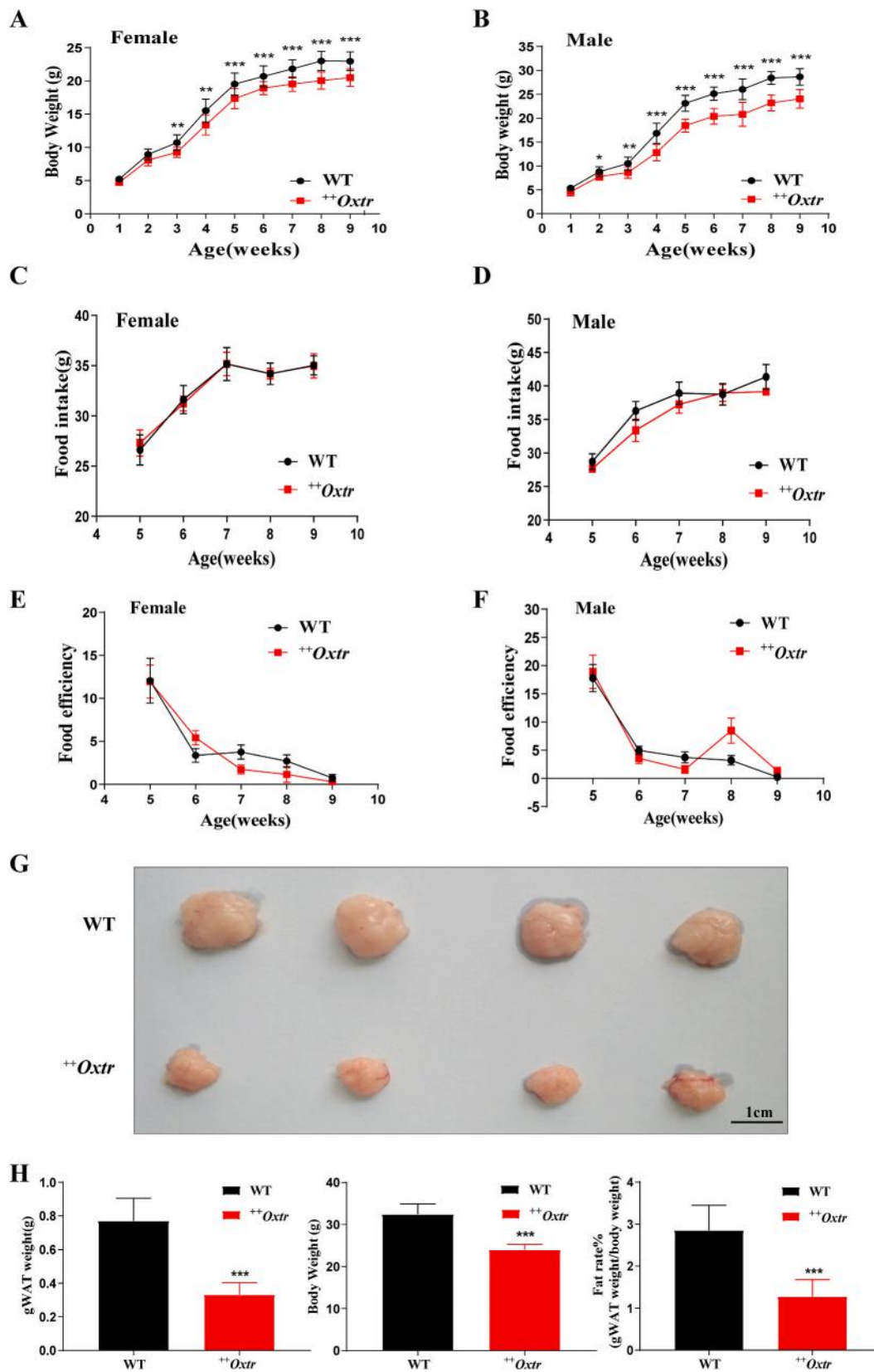


**Fig. 1.** *Oxtr* overexpression induces a lean phenotype of mice. WT and *++Oxtr* mice were on regular chow. Food intake and body weight were monitored weekly. (A–B) Time course of body weight of females (A) and males (B) from week 1–9 (n = 26–28). (C–D) Time course of food intake of females (C) and males (D) in each week from week 5–9 (n = 7–8). (E–F) Time course of food efficiency of females (E) and males (F) from week 5–9 (n = 7–8). (G) Representative macroscopic images of gWAT of males, scale bar: 1 cm. (H) gWAT weight, body weight and percentage body fat (gWAT weight/body weight × 100) of 16-week-old males (n = 4). \*\*\*P < 0.001, \*\*P < 0.01, \*P < 0.05.

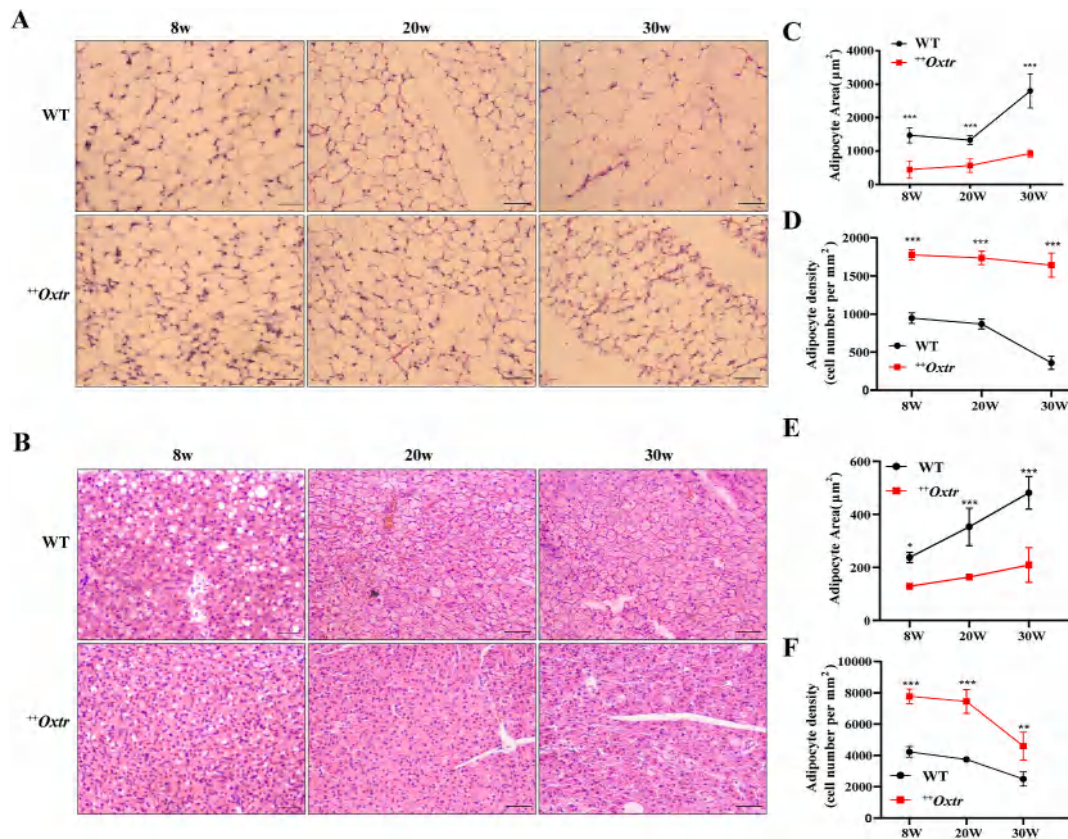


**Fig. 2.** *Oxtre* overexpression induces adipocyte browning. H&E-stained gWAT and BAT of 8-, 20-, 30-week-old males. (A–B) Representative H&E images of gWAT (A) and BAT (B), scale bar: 50 µm. (C–F) Cell size and density of gWAT (C and D) and BAT (E and F) per microscopic field ( $n = 3$ ). \*\*\* $P < 0.001$ , \*\* $P < 0.01$ , \* $P < 0.05$ .

littermates. To accurately assess the difference, food intake and body weight were monitored weekly for 9 weeks. Both female and male <sup>+/+</sup>*Oxtre* mice displayed significant lower body weight (95 % CI: -2.244 to -1.448 for females, -4.094 to -3.033 for males) compared to WT littermates starting at week 3 (Fig. 1A and B). No notable changes in food intake or efficiency were observed (Fig. 1C–F), indicating that the weight loss was not due to reduced caloric intake. Dissection analysis confirmed reduced gWAT mass in <sup>+/+</sup>*Oxtre* males (Fig. 1G and H), suggesting diminished fat accumulation, rather than appetite, as the primary driver of leanness.

### 3.2. *Oxtre* overexpression induces adipocyte browning

A reduction in adipocyte size, indicative of adipocyte browning, contrasts with an increase in size, known as hypertrophy [23]. Histological analysis of gWAT and BAT in 8-, 20-, 30-week-old males showed smaller adipocytes with multilocular lipid droplets in <sup>+/+</sup>*Oxtre* gWAT compared to WT. It appears that <sup>+/+</sup>*Oxtre* gWAT underwent a significant morphological transformation toward a BAT-like phenotype (Fig. 2A). BAT in WT mice gradually whitened and adipocytes became larger with age, while this phenomenon was not happening in <sup>+/+</sup>*Oxtre* BAT (Fig. 2B). Additionally, both gWAT and BAT of <sup>+/+</sup>*Oxtre* mice displayed reduced adipocyte size and increased cell density compared to WT (Fig. 2A and B), with the statistically significant difference in H&E staining (Fig. 2C–F). Overall, adipocyte browning in <sup>+/+</sup>*Oxtre* mice may lead to increased energy consumption, reduced gWAT mass and body weight loss.

### 3.3. *Oxtre* overexpression promotes energy metabolism

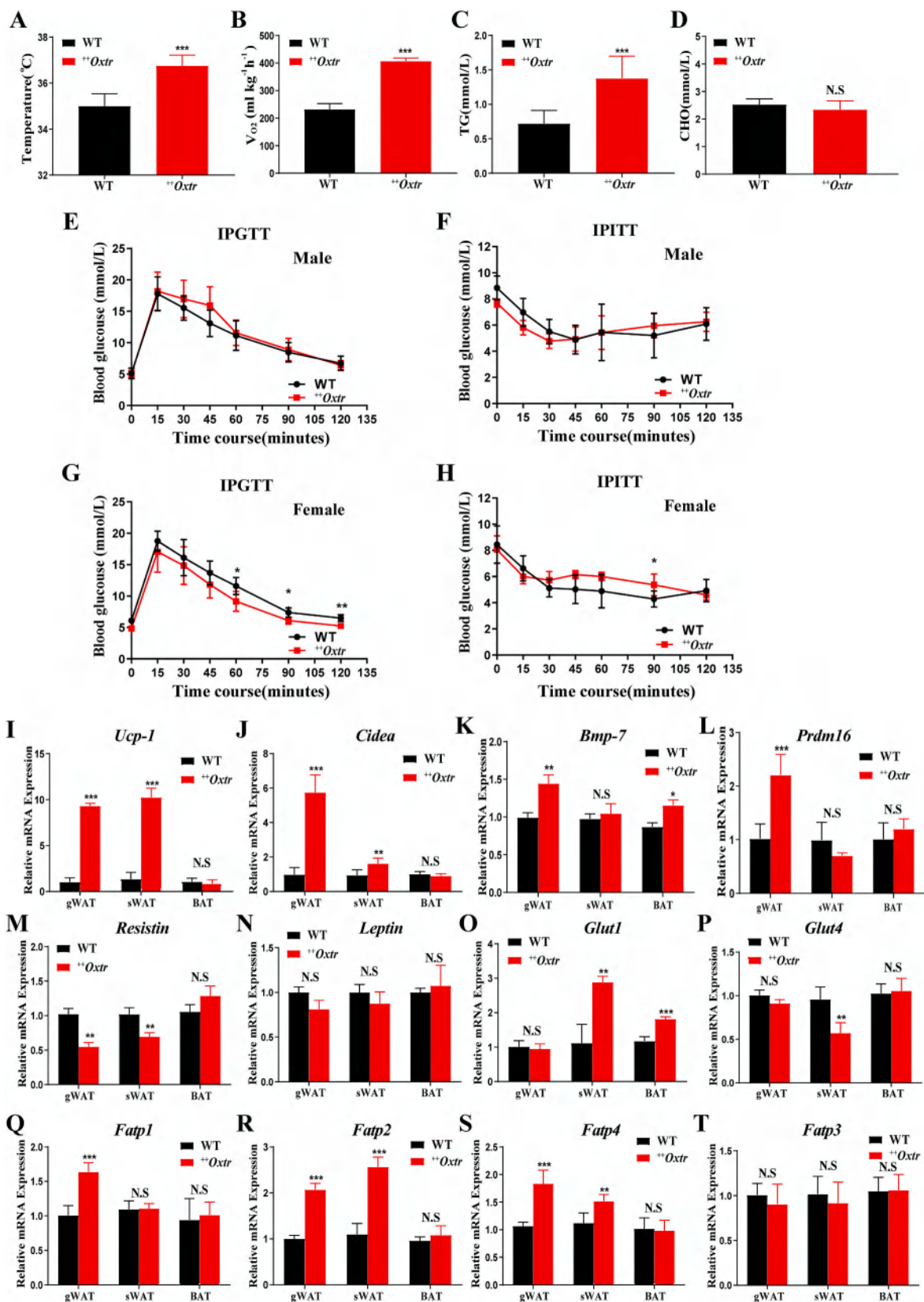
To further examine the difference in energy metabolism between WT and <sup>+/+</sup>*Oxtre* mice, we performed a cold tolerance test (4 °C) to assess

adaptive thermogenesis. <sup>+/+</sup>*Oxtre* males exhibited greater adaptive thermogenesis (95 % CI: 1.022 to 2.478) than WT males (Fig. 3A). Increased oxygen consumption of <sup>+/+</sup>*Oxtre* males indicates a faster metabolism and more energy loss in the form of heat (95 % CI: 143.0 to 206.9) compared to WT males (Fig. 3B). These effects support the lean phenotype induced by *Oxtre* overexpression. Fasting serum triglyceride were significantly elevated in <sup>+/+</sup>*Oxtre* males (Fig. 3C), but total cholesterol levels were unchanged (Fig. 3D). While no significant difference in intraperitoneal glucose and insulin tolerance test (IPGTT/IPITT) were detected between the WT and <sup>+/+</sup>*Oxtre* males (Fig. 3E and F), <sup>+/+</sup>*Oxtre* females exhibited improved glucose tolerance (Fig. 3G and H).

To investigate the significance of *Oxtre* overexpression on adipose development and function, the expression levels of key regulators of adipose tissue were assessed. Gene expression analysis demonstrated increased expression of BAT markers *Ucp-1*, *Cidea*, *Bmp7* and *Prmd16* in <sup>+/+</sup>*Oxtre* gWAT, while *Ucp-1* and *Cidea* were also upregulated in sWAT (Fig. 3I–L). *Resistin*, a WAT marker, exhibited decreased expression in <sup>+/+</sup>*Oxtre* gWAT and sWAT (Fig. 3M), supporting the WAT browning. *Leptin* expression was unaffected (Fig. 3N). Additionally, glucose transporter *Glut1* was upregulated, indicating an enhanced glucose uptake in <sup>+/+</sup>*Oxtre* adipocytes, whereas *Glut4* decreased in <sup>+/+</sup>*Oxtre* sWAT (Fig. 3O and P). Fatty acid transporters *Fatp1*, *Fatp2*, and *Fatp4* were elevated in <sup>+/+</sup>*Oxtre* WAT, while *Fatp3* levels remained unchanged (Fig. 3Q–T), supporting enhanced lipid metabolism. These findings support the notion that *Oxtre* overexpression induces alterations in gene expression, change in cell morphology and function in adipose tissues towards increased energy metabolism.

### 3.4. *Oxtre* overexpression protects mice against HFD-induced obesity and adipocyte whitening

To assess resistance to HFD-induced obesity, 3-week-old males were



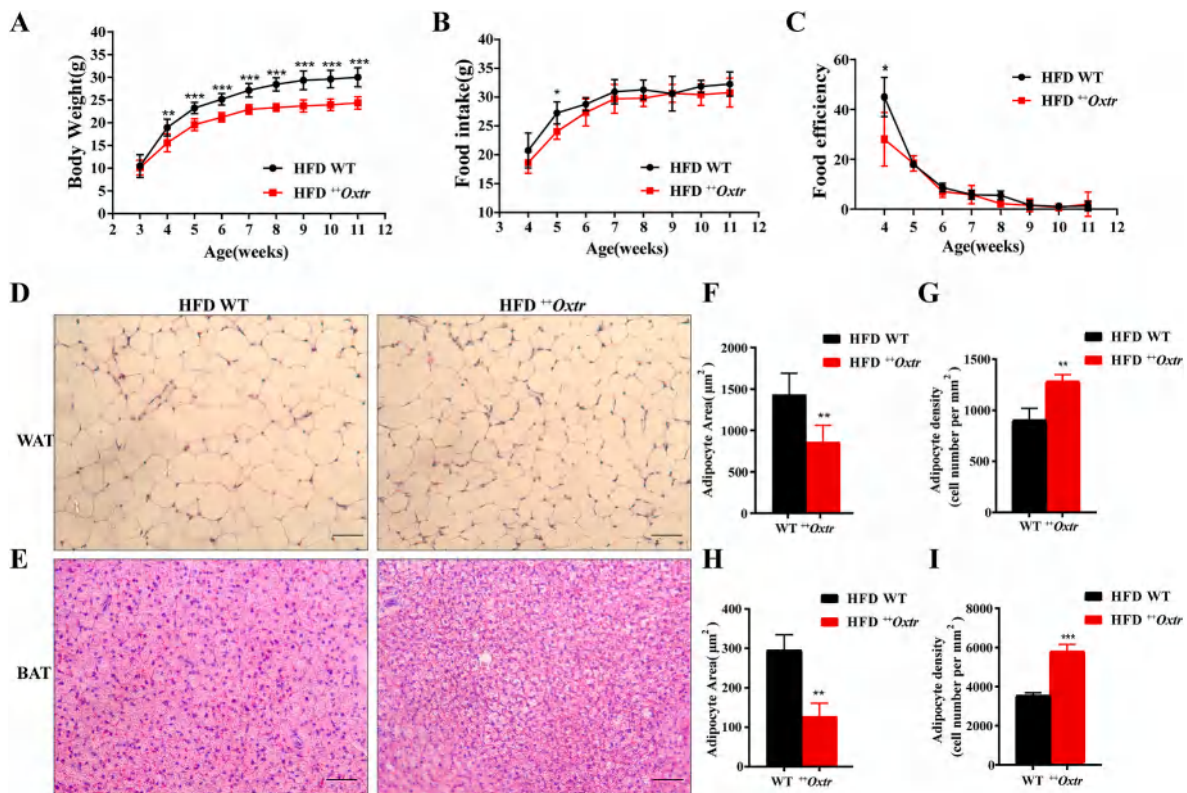


**Fig. 4.** *Oxtr* overexpression provides protection against obesity and brown fat whitening induced by HFD. WT and  $^{++}Oxtr$  males were fed an HFD for 2 months. (A) Time course of body weight of HFD-fed males from week 3–11 ( $n = 6$ ). (B) Time course of daily food intake of HFD-fed males from week 4–11 ( $n = 6$ ). (C) Time course of food efficiency of males from week 4–11 ( $n = 6$ ). (D–I) H&E staining of gWAT and BAT of 11-week-old males after an HFD. Representative images of gWAT (D) and BAT (E), scale bar: 50  $\mu\text{m}$ . Cell size and density of gWAT (F and G) and BAT (H and I) per microscopic field ( $n = 3$ ). \*\*\* $P < 0.001$ , \*\* $P < 0.01$ , \* $P < 0.05$ . (For interpretation of the references to colour in this figure legend, the reader is referred to the Web version of this article.)

fed an HFD for 2 months. With time, body weight gain of  $^{++}Oxtr$  males remained significantly lower (95 % CI:  $-4.672$  to  $-3.657$ ) than WT (Fig. 4A), despite comparable food intake and efficiency (Fig. 4B and C). Histologically,  $^{++}Oxtr$  gWAT displayed smaller adipocyte size but increased density compared to WT (Fig. 4D). As expected, the  $^{++}Oxtr$  BAT had a similar browning effect (Fig. 4E). Quantitative H&E analysis confirmed these morphological differences (Fig. 4F–I). Furthermore, HFD-induced hepatic lipid accumulation and lesions were milder in  $^{++}Oxtr$  mice than in WT controls (Fig. S2). These findings suggest that *Oxtr* overexpression confers a protective effect against HFD-induced obesity and adipocyte whitening.

### 3.5. *Oxtr* overexpression mitigates HFD-induced metabolic disorder

Under HFD conditions, a cold tolerance test was performed to assess adaptive thermogenesis. It is consistent with our previous results that HFD-fed  $^{++}Oxtr$  males displayed enhanced body temperature (95 % CI: 1.081 to 2.186) (Fig. 5A). This suggests that even under HFD-fed conditions,  $^{++}Oxtr$  males maintain a stronger metabolic capacity, leading to increased heat production. Higher insulin levels were observed in HFD-fed  $^{++}Oxtr$  males (95 % CI: 43.99 to 412.9) (Fig. 5B), suggesting that *Oxtr* overexpression increased insulin secretion in response to HFD-induced metabolic stress. Glucose tolerance was superior in HFD-fed  $^{++}Oxtr$  males (95 % CI:  $-3.467$  to  $-2.168$ ), with minimal changes in blood glucose levels (Fig. 5C), though insulin tolerance remained unchanged (Fig. 5D). *Oxtr* overexpression protects against HFD-induced metabolic disorder.

BAT markers (*Ucp-1* and *Cidea*) were markedly increased in gWAT and sWAT of HFD-fed  $^{++}Oxtr$  males (Fig. 5E and F), while *Bmp7* and *Prdm16* were up-regulated in sWAT and BAT (Fig. 5G and H). *Resistin* downregulation in gWAT, sWAT and BAT of  $^{++}Oxtr$  males supported the

anti-whitening effect (Fig. 5I). *Leptin*, *Fatp3* and *Fatp4* expression remained unaffected (Fig. 5J–L). Overall, the anti-obesity effect in  $^{++}Oxtr$  mice can be attributed to the upregulation of BAT markers, as well as enhanced metabolic capacity and glucose utilization.

### 3.6. *OXTR* overexpression induces the activation of PPAR signaling

Mechanistically, RNA sequencing was utilized to identify 365 differentially expressed genes (DEGs) of  $^{++}Oxtr$  against WT gWAT (286 upregulated and 79 downregulated) (Fig. S3). The heatmap of DEGs revealed upregulation of genes linked to carbohydrate digestion and absorption (PPAR pathway), alongside downregulation of steroid hormone biosynthesis-related genes in  $^{++}Oxtr$  gWAT (Fig. 6A). KEGG analysis showed that DEG enrichment in IL-17 pathways, PPAR signaling, unsaturated fatty acid biosynthesis, fatty acid elongation, and amino acid metabolism (Fig. 6B). Overlap analysis between  $^{++}Oxtr$  DEGs and PPAR $\gamma$ -bound genes identified 151 genes (41.3 % of DEGs) associated with fatty acid oxidation, amino acid metabolism, and calcium ion transport (Fig. 6C). PPAR $\gamma$  targets were upregulated in  $^{++}Oxtr$  gWAT (Fig. 6D and E), including *Fatp1*, *Resistin*, *Acaa1b*, *Fabp5*, *Apoc3*, *Glut4* and *Acot1*, which showed clear enrichment for PPAR $\gamma$  binding (Fig. 6F). These results suggest PPAR pathway activation underlies *OXTR*-driven adipocyte browning and enhanced energy metabolism.

## 4. Discussion

Oxytocin Receptor (*OXTR*) is well-known for its involvement in various biological processes, including social bonding, mammary gland development and cancers [8,9,24]. *Oxtr*-knockout mice (*Oxtr* $^{-/-}$ ) develop obesity and diabetes characterized by enlarged adipocyte sizes and hypertrophy in epididymal fat pads, highlighting its role in energy

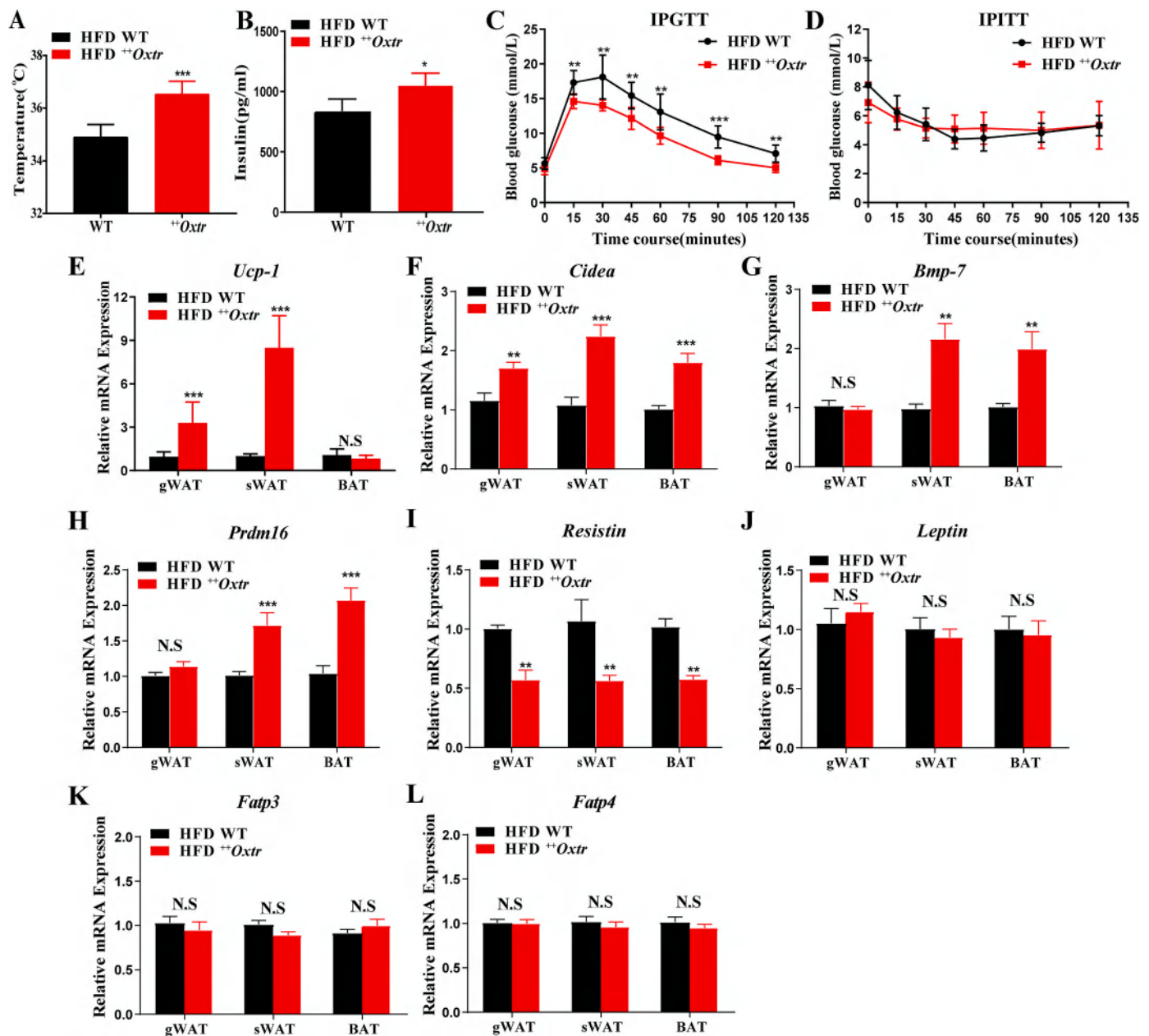


**Fig. 5.** *OxtR* overexpression protects against HFD-induced metabolic disorder. (A) Body temperature of HFD-fed <sup>+/+</sup>*OxtR* and WT males at 4 °C for 4 h (n = 6). (B) Serum insulin levels in HFD-fed <sup>+/+</sup>*OxtR* and WT males (n = 5). (C) IPGTT of HFD-fed 11-week-old males fasted for 16 h (n = 5). (D) IPITT of HFD-fed 11-week-old males fasted for 4 h (n = 5). (E–L) Relative mRNA levels of BAT marker genes (E–H), WAT marker genes (I–J), and fatty acid transport related genes (K–L) in gWAT, sWAT and BAT of males, normalized against 18S (n = 4). \*\*\*P < 0.001, \*\*P < 0.01, \*P < 0.05, N.S., not significant.

metabolism [12,14]. Oxytocin signaling within the posterior hypothalamus exerts a protective effect against hyperphagic obesity in murine models [7]. Additionally, oxytocin enhances thermogenesis and mitigates obesity and metabolic disorders by promoting WAT browning and stimulating thermogenesis in BAT, WAT and skeletal muscle [15,16]. However, the metabolic consequences of OXTR overexpression remain poorly understood. In our study, transgenic mice overexpression OXTR under the  $\beta$ -actin promoter (<sup>+/+</sup>*OxtR*) were utilized. Our findings demonstrate *OxtR* overexpression effectively prevents obesity and metabolic dysfunction by enhancing adaptive thermogenesis, increasing energy consumption and improving glucose tolerance. Molecular analyses revealed *OxtR* overexpression activates the PPAR signaling pathway, a key regulator of energy metabolism.

*OxtR*<sup>-/-</sup> and *OxtR*<sup>-/-</sup> mice develop late-onset obesity without changes in food intake [14,25–27]. In contrast, <sup>+/+</sup>*OxtR* mice exhibited a leaner

phenotype with reduced gWAT mass, despite comparable daily food intake to WT mice. Additionally, *OxtR* overexpression conferred resistance to HFD-induced obesity and adipocyte whitening. <sup>+/+</sup>*OxtR* adipose tissues displayed a morphological shift toward a BAT-like phenotype, marked by smaller, multilocular adipocytes. BAT, which is rich in mitochondria, utilizes fatty acids and glucose for thermogenesis through UCP1-mediated mitochondrial respiration [28]. UCP1, a BAT-specific protein located in the inner mitochondrial membrane, is essential for thermogenesis. The enhanced thermogenesis and oxygen consumption observed in <sup>+/+</sup>*OxtR* mice suggest accelerated metabolism and greater energy expenditure, consistent with their lean phenotype. Future studies could explore BAT and WAT responses to  $\beta$ -adrenergic stimulation or cold exposure in OXTR-overexpressing models to elucidate thermogenic pathways. While *OxtR*<sup>-/-</sup> mice develop normally, they display glucose resistance and impaired insulin secretion under HFD conditions [29]. In

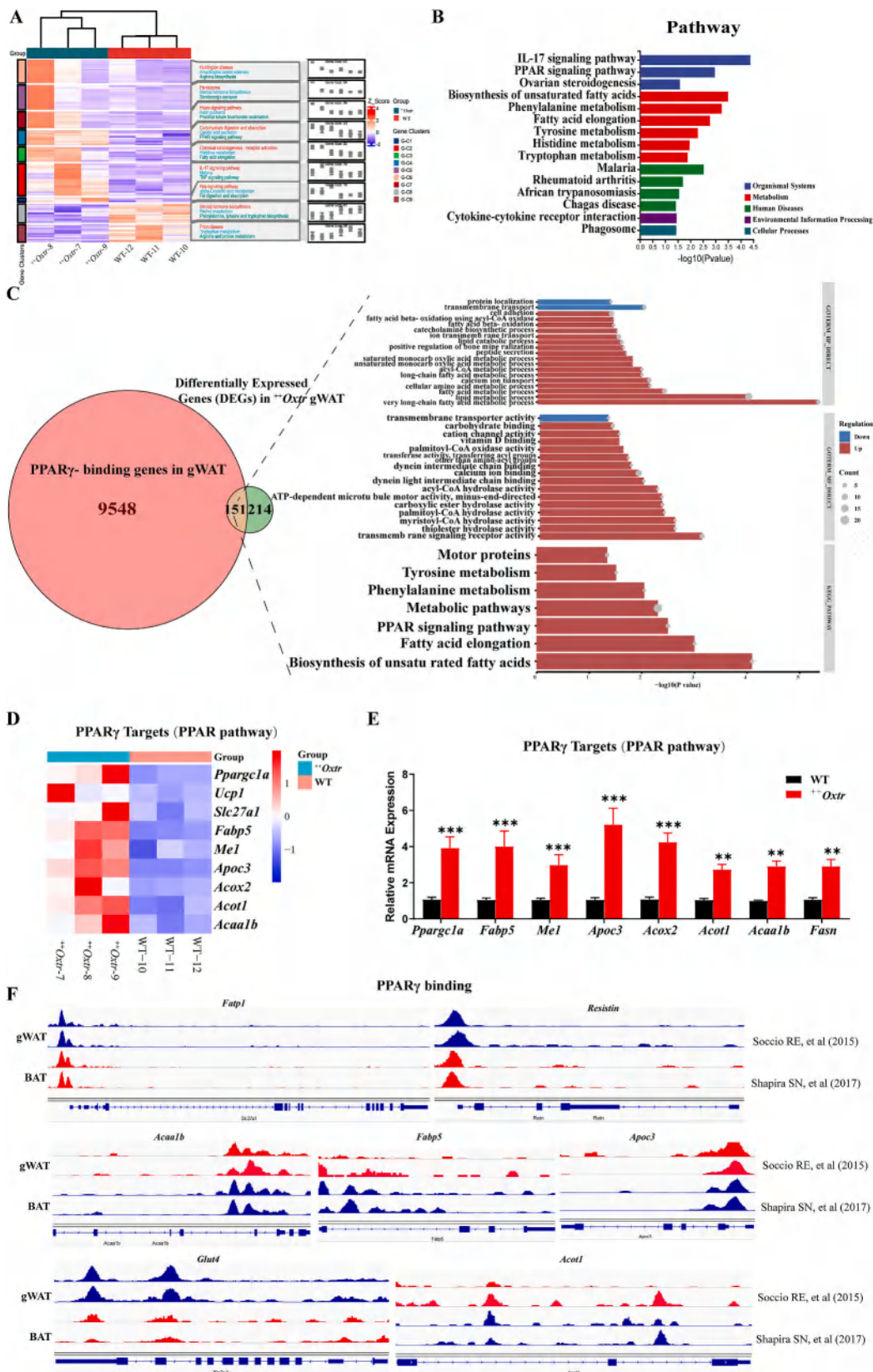


**Fig. 6.** OXTR overexpression activates PPAR signaling pathway.  $^{++}Oxtr$  and WT gWAT from 8-week-old males were subjected for RNA sequencing. (A) The heatmap displayed gene expression patterns of DEGs in  $^{++}Oxtr$  and WT gWAT. (B) KEGG enrichment analysis of DEGs between  $^{++}Oxtr$  and WT gWAT. (C) The venn diagram showed the overlap between PPAR $\gamma$ -binding genes [55] (Data from GSM1571716 were re-analyzed) and DEGs between  $^{++}Oxtr$  and WT gWAT. GO analysis of overlapping genes. (D) The heatmap displayed gene expression patterns of PPAR $\gamma$  targets (PPAR pathway) in  $^{++}Oxtr$  and WT gWAT. (E) Relative mRNA levels of PPAR $\gamma$  targets in gWAT of males, normalized against 18S (n = 3). (F) ChIP-seq profiles of PPAR $\gamma$  enrichment on *Fatp1*, *Resistin*, *Acaa1b*, *Fabp5*, *Apoc3*, *Glut4* and *Acot1* in mouse gWAT [55] and BAT [56] (Data from GSM1571716, GSM1571715, GSM2551928, GSM2551929 were obtained).

our study, HFD-fed <sup>++</sup>*Oxtr* mice demonstrated enhanced insulin secretion and superior glucose tolerance compared to HFD-fed WT mice. Although systemic insulin tolerance showed no significant differences, *Oxtr* overexpression may improve  $\beta$ -cell survival or glucose sensing, facilitating efficient insulin release and glucose uptake. Additionally, HFD-induced hepatic lipid accumulation and lesions were milder in <sup>++</sup>*Oxtr* mice than in WT controls, suggesting that non-adipose tissues (e.g., liver, pancreas) contribute to the metabolic benefits of systemic OXTR overexpression. These effects appear context-dependent and influenced by genetic factors rather than dietary modulation.

Mechanistically, OXTR overexpression activated PPAR signaling, a central regulator of energy homeostasis. PPARs, a family of fatty acid-activated nuclear receptors, include three subtypes: PPAR $\alpha$ , PPAR $\delta$ , and PPAR $\gamma$  [30–32]. PPAR $\alpha$  and PPAR $\delta$  are abundant in oxidative tissues and regulate genes involved in oxidative phosphorylation, substrate delivery, and energy homeostasis [33]. In contrast, PPAR $\gamma$ , highly expressed in WAT and BAT, governs adipocyte differentiation and lipid metabolism [34,35]. It also induces thermogenic and mitochondrial biogenesis genes, such as *Ucp1*, *Pgc1 $\alpha$* , and *Prdm16* [36,37]. PPAR $\gamma$  activation promotes WAT browning via a SIRT1-PPAR $\gamma$ -PRDM16 cascade [38], ameliorating insulin resistance by suppressing WAT-specific genes (e.g., *Resistin*) and upregulating BAT markers (e.g., *Ucp1* and *Cidea*) [39,40]. Our study confirmed elevated expression of brown adipocytes markers (*Ucp1*, *Bmp7*, *Prdm16*, and *Cidea*) and reduced *Resistin* in WAT, strongly supporting OXTR-driven adipocyte browning and thermogenesis via PPAR pathway.

PPAR $\gamma$  enhances fatty acid uptake, triglyceride storage, glucose metabolism and insulin sensitivity. Adipose-specific PPAR $\gamma$  deletion causes lipodystrophy and metabolic dysfunction, emphasizing its role in adipocyte function [41,42]. PPAR $\gamma$  also upregulates fatty acid transporters (e.g., FATPs) to promote oxidation [43,44]. We have identified that 41.3 % of DEGs in <sup>++</sup>*Oxtr* WAT are PPAR $\gamma$  targets associated with fatty acid oxidation, amino acid metabolism, and calcium ion transport. Key PPAR $\gamma$ -targets, including *Fatp1*, *Fatp2*, *Glut1*, *Acaa1b* and *Acox2*, were upregulated, while *Resistin* was downregulated in <sup>++</sup>*Oxtr* adipose tissue. *Fatp1* enhances fatty acid uptake [45] and mitochondrial oxidation [46], while *Fatp1* and *Fatp2* contribute to thermogenesis [47]. PPAR $\gamma$  agonists improve glucose uptake by *Glut1* induction, aligning with superior glucose tolerance in <sup>++</sup>*Oxtr* mice. However, *Glut4* expression was decreased in sWAT, a paradoxical finding given its role in adipocyte glucose transport. [28,29]. *Glut4* protein in WAT is decreased in obese or lean rats [48]. *Acaa1* and *Acox2*, which catalyze  $\beta$ -oxidation and fatty acid degradation, likely enhance lipid metabolism and reduce fat deposition [49,50]. Collectively, these findings provide strong evidence that OXTR activation improves lipid metabolism and glucose homeostasis via PPAR pathway. Oxytocin treatment induced adipocytes shrinkage and PPAR $\gamma$  upregulation in gWAT [51]. Our study confirms OXTR overexpression activates PPAR signaling which contributes to energy metabolism, indicating the activation effects of OXTR/OXTR system on PPAR signaling.

OXTR agonists are under investigation for autism spectrum disorder, Alzheimer's disease, anxiety disorders and depression. However, brain-specific delivery systems (e.g., nanoparticle carriers) may mitigate peripheral side effects [52]. Topical OXTR agonists could offer targeted analgesia without central nervous system (CNS) penetration, minimizing systemic risks [53]. Furthermore, epigenetic modulation of OXTR expression (e.g., via DNA methyltransferase inhibitors) could restore receptor function in disorders linked to OXTR methylation, such as childhood trauma-related psychopathologies [54].

Despite therapeutic potential, OXTR overexpression or off-target activation poses risks. For instance, universal OXTR overexpression disrupts progesterone and prolactin signaling, resulting in precocious mammary gland development, milk production and HER2+ tumors in non-pregnant females, as well as lactation failure via prolactin/p-STAT5 pathway activation [8,9]. Males may be more inclined to utilize targeted therapy due to hormonal changes in females influenced by OXTR. These

findings highlight the need for tissue-specific OXTR targeting to avoid metabolic or oncogenic complications. Screening for OXTR expression and epigenetic status may identify at-risk individuals. Future research should prioritize context-dependent OXTR roles and long-term safety in translational models.

## 5. Conclusions

Using the <sup>++</sup>*Oxtr* mouse model, we elucidated OXTR's role in energy metabolism and adipose remodeling. OXTR overexpression induces the activation of PPAR signaling, which contributes to the amelioration of obesity and metabolic disorders through WAT browning, increased energy metabolism, enhanced adaptive thermogenesis. The effects of OXTR are highly context-dependent, and driven by nonspecific genetic rather than dietary factors.

## CRedit authorship contribution statement

**Xinyue Bao:** Writing – original draft, Methodology, Conceptualization. **Mingjun San:** Writing – original draft, Methodology, Conceptualization. **Shuilian Wang:** Formal analysis, Data curation. **Yanli Zhuo:** Resources. **Ziyang Liu:** Formal analysis, Data curation. **Yaowu Zheng:** Writing – review & editing, Methodology, Conceptualization. **Dan Li:** Writing – review & editing, Methodology, Conceptualization.

## Institutional review board statement

The Ethics Committee of Shenyang Medical College registered and authorized all research studies and protocols (SYXY2023061001), which followed the ethical standards stated in the Guidance on the operation of the Animals (Scientific Procedures) and National Institutes of Health's Guide for Care and Use of Laboratory Animals.

## Data accessibility

The RNA sequencing data has been deposited in the GEO database (accession numbers: GSE276520). All data presented are available from the corresponding author.

## Declaration of competing interest

All authors have seen and approved the final version of the manuscript being submitted. The article is the authors' original work, hasn't received prior publication and isn't under consideration for publication elsewhere.

All authors declare that they have no known competing financial interests or personal relationships that could have appeared to influence the work reported in this paper.

## Acknowledgements

This work is supported by National Natural Science Foundation of China (82103188), Natural Science Foundation of Liaoning Province, China (2023-MS-325, LJKZ1148) and Undergraduate Innovation and Entrepreneurship Training Program (20249007). The above fundings were used for the purchase of materials and reagents, RNA sequencing and the feeding of mice.

## Appendix A. Supplementary data

Supplementary data to this article can be found online at <https://doi.org/10.1016/j.yexcr.2025.114534>.

## Data availability

Data will be made available on request.

## References

- [1] S.-C. Chien, C. Chandramouli, C.-I. Lo, C.-F. Lin, K.-T. Sung, W.-H. Huang, Y.-H. Lai, C.-H. Yun, C.-H. Su, H.-I. Yeh, T.-C. Hung, C.-L. Hung, C.S.P. Lam, Associations of obesity and malnutrition with cardiac remodeling and cardiovascular outcomes in Asian adults: a cohort study, *PLoS Med.* 18 (2021) e1003661, <https://doi.org/10.1371/journal.pmed.1003661>.
- [2] F. Zhang, G. Hao, M. Shao, K. Nham, Y. An, Q. Wang, Y. Zhu, C.M. Kusminski, G. Hassan, R.K. Gupta, Q. Zhai, X. Sun, P.E. Scherer, O.K. Oz, An adipose tissue atlas: an image-guided identification of human-like BAT and beige depots in rodents, *Cell Metab.* 27 (2018) 252–262.e3, <https://doi.org/10.1016/j.cmet.2017.12.004>.
- [3] M. Chondronikola, E. Volpi, E. Børsheim, C. Porter, M.K. Saraf, P. Annamalai, C. Yfanti, T. Chao, D. Wong, K. Shinoda, S.M. Labbé, N.M. Hurren, F. Cesani, S. Kajimura, L.S. Sidossis, Brown adipose tissue activation is linked to distinct systemic effects on lipid metabolism in humans, *Cell Metab.* 23 (2016) 1200–1206, <https://doi.org/10.1016/j.cmet.2016.04.029>.
- [4] X. Liu, S. Wang, Y. You, M. Meng, Z. Zheng, M. Dong, J. Lin, Q. Zhao, C. Zhang, X. Yuan, T. Hu, L. Liu, Y. Huang, L. Zhang, D. Wang, J. Zhan, H. Jong Lee, J. R. Speakman, W. Jin, Brown adipose tissue transplantation reverses obesity in ob/ob mice, *Endocrinology* 156 (2015) 2461–2469, <https://doi.org/10.1210/en.2014-1598>.
- [5] Y. Takayanagi, M. Yoshida, I.F. Bielsky, H.E. Ross, M. Kawamata, T. Onaka, T. Yanagisawa, T. Kimura, M.M. Matzuk, L.J. Young, K. Nishimori, Pervasive social deficits, but normal parturition, in oxytocin receptor-deficient mice, *Proc. Natl. Acad. Sci. U. S. A.* 102 (2005) 16096–16101, <https://doi.org/10.1073/pnas.0505312102>.
- [6] J.S. Carter, S.K. Wood, A.M. Kearns, J.L. Hopkins, C.M. Reichel, Paraventricular nucleus of the hypothalamus oxytocin and incubation of heroin seeking, *Neuroendocrinology* 113 (2023) 1112–1126, <https://doi.org/10.1159/000529358>.
- [7] K. Inada, K. Tsujimoto, M. Yoshida, K. Nishimori, K. Miyamichi, Oxytocin signaling in the posterior hypothalamus prevents hyperphagic obesity in mice, *Elife* 11 (2022) e75718, <https://doi.org/10.7554/eLife.75718>.
- [8] D. Li, Y. Ji, C. Zhao, Y. Yao, A. Yang, H. Jin, Y. Chen, M. San, J. Zhang, M. Zhang, L. Zhang, X. Feng, Y. Zheng, OXTR overexpression leads to abnormal mammary gland development in mice, *J. Endocrinol.* 239 (2018) 121–136, <https://doi.org/10.1530/JOE-18-0356>.
- [9] D. Li, M. San, J. Zhang, A. Yang, W. Xie, Y. Chen, X. Lu, Y. Zhang, M. Zhao, X. Feng, Y. Zheng, Oxytocin receptor induces mammary tumorigenesis through prolactin/p-STAT5 pathway, *Cell Death Dis.* 12 (2021) 588, <https://doi.org/10.1038/s41419-021-03849-8>.
- [10] I. Papazoglou, J.-H. Lee, Z. Cui, C. Li, G. Fulgenzi, Y.J. Bahn, H.M. Staniszevska-Goraczniak, R.A. Piñol, I.B. Hogue, L.W. Enquist, M.J. Krashes, S.G. Rane, A distinct hypothalamus-to- $\beta$  cell circuit modulates insulin secretion, *Cell Metab.* 34 (2022) 285–298.e7, <https://doi.org/10.1016/j.cmet.2021.12.020>.
- [11] C. Camerino, E. Conte, R. Caloiero, A. Fonzino, M. Carrath, M.D. Lograno, D. Tricarico, Evaluation of Short and long term cold stress challenge of nerve growth factor, brain-derived neurotrophic factor, osteocalcin and oxytocin mRNA expression in BAT, brain, bone and reproductive tissue of male mice using real-time PCR and linear correlation analysis, *Front. Physiol.* 8 (2018), <https://doi.org/10.3389/fphys.2017.01101>.
- [12] Y. Takayanagi, Y. Kasahara, T. Onaka, N. Takahashi, T. Kawada, K. Nishimori, Oxytocin receptor-deficient mice developed late-onset obesity, *Neuroreport* 19 (2008) 951, <https://doi.org/10.1097/WNR.0b013e3283021ca9>.
- [13] Y. Kasahara, Y. Tateishi, Y. Hiraoka, A. Otsuka, H. Mizukami, K. Ozawa, K. Sato, S. Hidema, K. Nishimori, Role of the oxytocin receptor expressed in the rostral medullary raphe in thermoregulation during cold conditions, *Front. Endocrinol.* 6 (2015), <https://doi.org/10.3389/fendo.2015.00180>.
- [14] C. Camerino, Low sympathetic tone and obese phenotype in oxytocin-deficient mice, *Obesity* 17 (2009) 980–984, <https://doi.org/10.1038/oby.2009.12>.
- [15] J. Yuan, R. Zhang, R. Wu, Y. Gu, Y. Lu, The effects of oxytocin to rectify metabolic dysfunction in obese mice are associated with increased thermogenesis, *Mol. Cell. Endocrinol.* 514 (2020) 110903, <https://doi.org/10.1016/j.mce.2020.110903>.
- [16] L. Sun, D. Lizneva, Y. Ji, G. Colaianni, E. Hadelia, A. Gumerova, K. Ievleva, T.-C. Kuo, F. Korkmaz, V. Ryu, A. Rahimova, S. Gera, C. Taneja, A. Khan, N. Ahmad, R. Tamma, Z. Bian, A. Zallone, S.-M. Kim, M.I. New, J. Iqbal, T. Yuen, M. Zaidi, Oxytocin regulates body composition, *Proc. Natl. Acad. Sci. U. S. A.* 116 (2019) 26808–26815, <https://doi.org/10.1073/pnas.1913611116>.
- [17] M. Malumbres, R. Mangués, N. Ferrer, S. Lu, A. Pellicer, Isolation of high molecular weight DNA for reliable genotyping of transgenic mice, *Biotechniques* 22 (1997) 1114–1119, <https://doi.org/10.2144/97226st03>.
- [18] P.N. Marshall, R.W. Horobin, The mechanism of action of “mordant” dyes—a study using preformed metal complexes, *Histochemie* 35 (1973) 361–371, <https://doi.org/10.1007/BF00310675>.
- [19] J.A. Ramos-Vara, Technical aspects of immunohistochemistry, *Vet. Pathol.* 42 (2005) 405–426, <https://doi.org/10.1354/vp.42-4-405>.
- [20] C.-Y. Shi, H. Yang, C.-L. Wei, O. Yu, Z.-Z. Zhang, C.-J. Jiang, J. Sun, Y.-Y. Li, Q. Chen, T. Xia, X.-C. Wan, Deep sequencing of the *Camellia sinensis* transcriptome revealed candidate genes for major metabolic pathways of tea-specific compounds, *BMC Genom.* 12 (2011) 131, <https://doi.org/10.1186/1471-2164-12-131>.
- [21] C. Trapnell, A. Roberts, L. Goff, G. Pertea, D. Kim, D.R. Kelley, H. Pimentel, S. L. Salzberg, J.L. Rinn, L. Pachter, Differential gene and transcript expression analysis of RNA-seq experiments with TopHat and Cufflinks, *Nat. Protoc.* 7 (2012) 562–578, <https://doi.org/10.1038/nprot.2012.016>.
- [22] Y. Benjamini, D. Drai, G. Elmer, N. Kafkafi, I. Golani, Controlling the false discovery rate in behavior genetics research, *Behav. Brain Res.* 125 (2001) 279–284, [https://doi.org/10.1016/s0166-4328\(01\)00297-2](https://doi.org/10.1016/s0166-4328(01)00297-2).
- [23] T. Karpanen, M. Bry, H.M. Ollila, T. Seppänen-Laakso, E. Liimatta, H. Leskinen, R. Kivelä, T. Helkamaa, M. Merentie, M. Jeltsch, K. Paavonen, L.C. Andersson, E. Mervaala, I.E. Hassinen, S. Ylä-Herttuala, M. Orešič, K. Alitalo, Overexpression of vascular endothelial growth factor-B in mouse heart alters cardiac lipid metabolism and induces myocardial hypertrophy, *Circ. Res.* 103 (2008) 1018–1026, <https://doi.org/10.1161/CIRCRESAHA.108.178459>.
- [24] G. Leng, N. Sabatier, Oxytocin - the sweet hormone? *Trends Endocrinol Metab* 28 (2017) 365–376, <https://doi.org/10.1016/j.tem.2017.02.007>.
- [25] R.C. Mantella, L. Rinaman, R.R. Vollmer, J.A. Amico, Cholecystokinin and D-fenfluramine inhibit food intake in oxytocin-deficient mice, *Am. J. Physiol. Regul. Integr. Comp. Physiol.* 285 (2003) R1037–R1045, <https://doi.org/10.1152/ajpregu.00383.2002>.
- [26] L. Rinaman, R.R. Vollmer, J. Karam, D. Phillips, X. Li, J.A. Amico, Dehydration anorexia is attenuated in oxytocin-deficient mice, *Am. J. Physiol. Regul. Integr. Comp. Physiol.* 288 (2005) R1791–R1799, <https://doi.org/10.1152/ajpregu.00860.2004>.
- [27] Y. Kasahara, K. Sato, Y. Takayanagi, H. Mizukami, K. Ozawa, S. Hidema, K.-H. So, T. Kawada, N. Inoue, I. Ikeda, S.-G. Roh, K. Itoi, K. Nishimori, Oxytocin receptor in the hypothalamus is sufficient to rescue normal thermoregulatory function in male oxytocin receptor knockout mice, *Endocrinology* 154 (2013) 4305–4315, <https://doi.org/10.1210/en.2012-2206>.
- [28] A. Sakers, M.K. De Siqueira, P. Seale, C.J. Villanueva, Adipose-tissue plasticity in health and disease, *Cell* 185 (2022) 419–446, <https://doi.org/10.1016/j.cell.2021.12.016>.
- [29] S. Watanabe, F.-Y. Wei, T. Matsunaga, N. Matsunaga, T. Kaitsuka, K. Tomizawa, Oxytocin protects against stress-induced cell death in murine pancreatic  $\beta$ -cells, *Sci. Rep.* 6 (2016) 25185, <https://doi.org/10.1038/srep25185>.
- [30] C. A. R. Jf, E. Rm, M. Dj, Nuclear receptors and lipid physiology: opening the X-files, *Science* (New York, N.Y.) 294 (2001), <https://doi.org/10.1126/science.294.5548.1866>.
- [31] T.M. Willson, P.J. Brown, D.D. Sternbach, B.R. Henke, The PPARs: from orphan receptors to drug discovery, *J. Med. Chem.* 43 (2000) 527–550, <https://doi.org/10.1021/jm990554g>.
- [32] B. Grygiel-Górniak, Peroxisome proliferator-activated receptors and their ligands: nutritional and clinical implications—a review, *Nutr. J.* 13 (2014) 17, <https://doi.org/10.1186/1475-2891-13-17>.
- [33] A. Christofides, E. Konstantinidou, C. Jani, V.A. Boussiotis, The role of peroxisome proliferator-activated receptors (PPAR) in immune responses, *Metabolism* 114 (2021) 154338, <https://doi.org/10.1016/j.metabol.2020.154338>.
- [34] A. M, S. Jm, H. N, L. C, A. Ar, D. M, E. Rm, PPAR $\gamma$  signaling and metabolism: the good, the bad and the future, *Nat. Med.* 19 (2013), <https://doi.org/10.1038/nm.3159>.
- [35] B. Cariou, B. Charbonnel, B. Staels, Thiazolidinediones and PPAR $\gamma$  agonists: time for a reassessment, *Trends in Endocrinology & Metabolism* 23 (2012) 205–215, <https://doi.org/10.1016/j.tem.2012.03.001>.
- [36] D. Moutaigne, L. Butruille, B. Staels, PPAR control of metabolism and cardiovascular functions, *Nat. Rev. Cardiol.* 18 (2021) 809–823, <https://doi.org/10.1038/s41569-021-00569-6>.
- [37] B. Gross, M. Pawlak, P. Lefebvre, B. Staels, PPARs in obesity-induced T2DM, dyslipidaemia and NAFLD, *Nat. Rev. Endocrinol.* 13 (2017) 36–49, <https://doi.org/10.1038/nrendo.2016.135>.
- [38] N. Petrovic, T.B. Walden, I.G. Shabalina, J.A. Timmons, B. Cannon, J. Nedergaard, Chronic peroxisome proliferator-activated receptor  $\gamma$  (PPAR $\gamma$ ) activation of epididymally derived white adipocyte cultures reveals a population of thermogenically competent, UCP1-containing adipocytes molecularly distinct from classic Brown adipocytes, *J. Biol. Chem.* 285 (2010) 7153–7164, <https://doi.org/10.1074/jbc.M109.053942>.
- [39] L. Qiang, L. Wang, N. Kon, W. Zhao, S. Lee, Y. Zhang, M. Rosenbaum, Y. Zhao, W. Gu, S.R. Farmer, D. Accili, Brown remodeling of white adipose tissue by SirT1-dependent deacetylation of Ppar $\gamma$ , *Cell* 150 (2012) 620–632, <https://doi.org/10.1016/j.cell.2012.06.027>.
- [40] R. Mayoral, O. Osborn, J. McNelis, A.M. Johnson, D.Y. Oh, C.L. Izquierdo, H. Chung, P. Li, P.G. Traves, G. Bandyopadhyay, A.R. Pessentheiner, J.M. Ofrecio, J.R. Cook, L. Qiang, D. Accili, J.M. Olefsky, Adipocyte SIRT1 knockout promotes PPAR $\gamma$  activity, adipogenesis and insulin sensitivity in chronic-HFD and obesity, *Mol Metab* 4 (2015) 378–391, <https://doi.org/10.1016/j.molmet.2015.02.007>.
- [41] J.A. Hall, D. Ramachandran, H.C. Roh, J.R. DiSpirito, T. Belchior, P.-J.H. Zushin, C. Palmer, S. Hong, A.I. Mina, B. Liu, Z. Deng, P. Aryal, C. Jacobs, D. Tenen, C. W. Brown, J.F. Charles, G.I. Shulman, B.B. Kahn, L.T.Y. Tsai, E.D. Rosen, B. M. Spiegelman, A.S. Banks, Obesity-linked PPAR $\gamma$  S273 phosphorylation promotes insulin resistance through Growth Differentiation Factor 3, *Cell Metab.* 32 (2020) 665–675.e6, <https://doi.org/10.1016/j.cmet.2020.08.016>.
- [42] F. Wang, S.E. Mullican, J.R. DiSpirito, L.C. Peed, M.A. Lazar, Lipatrophy and severe metabolic disturbance in mice with fat-specific deletion of PPAR $\gamma$ , *Proc. Natl. Acad. Sci. U. S. A.* 110 (2013) 18656–18661, <https://doi.org/10.1073/pnas.1314863110>.
- [43] J.I. Odegaard, R.R. Ricardo-Gonzalez, M.H. Goforth, C.R. Morel, V. Subramanian, L. Mukundan, A. Red Eagle, D. Vats, F. Brombacher, A.W. Ferrante, A. Chawla, Macrophage-specific PPAR $\gamma$  controls alternative activation and improves insulin resistance, *Nature* 447 (2007) 1116–1120, <https://doi.org/10.1038/nature05894>.
- [44] S. Liu, H. Zhang, Y. Li, Y. Zhang, Y. Bian, Y. Zeng, X. Yao, J. Wan, X. Chen, J. Li, Z. Wang, Z. Qin, S100A4 enhances protumor macrophage polarization by control

- of PPAR- $\gamma$ -dependent induction of fatty acid oxidation, *J Immunother Cancer* 9 (2021) e002548, <https://doi.org/10.1136/jitc-2021-002548>.
- [45] J. Huang, R. Zhu, D. Shi, The role of FATP1 in lipid accumulation: a review, *Mol. Cell. Biochem.* 476 (2021) 1897–1903, <https://doi.org/10.1007/s11010-021-04057-w>.
- [46] D. Sebastián, M. Guitart, C. García-Martínez, C. Mauvezin, J.M. Orellana-Gavaldà, D. Serra, A.M. Gómez-Foix, F.G. Hegardt, G. Asins, Novel role of FATP1 in mitochondrial fatty acid oxidation in skeletal muscle cells, *JLR (J. Lipid Res.)* 50 (2009) 1789–1799, <https://doi.org/10.1194/jlr.M800535-JLR200>.
- [47] R. Acharya, S.S. Shetty, S. Kumari N, Fatty acid transport proteins (FATPs) in cancer, *Chem. Phys. Lipids* 250 (2023) 105269, <https://doi.org/10.1016/j.chemphyslip.2022.105269>.
- [48] P.M. Seraphim, M.T. Nunes, U.F. Machado, GLUT4 protein expression in obese and lean 12-month-old rats: insights from different types of data analysis, *Braz. J. Med. Biol. Res.* 34 (2001) 1353–1362, <https://doi.org/10.1590/S0100-879X2001001000018>.
- [49] S. Zhu, S. Park, Y. Lim, S. Shin, S.N. Han, Korean pine nut oil replacement decreases intestinal lipid uptake while improves hepatic lipid metabolism in mice, *Nutr Res Pract* 10 (2016) 477–486, <https://doi.org/10.4162/nrp.2016.10.5.477>.
- [50] Y. Zhang, Y. Chen, Z. Zhang, X. Tao, S. Xu, X. Zhang, T. Zurashvili, Z. Lu, J. R. Bayascas, L. Jin, J. Zhao, X. Zhou, Acox2 is a regulator of lysine crotonylation that mediates hepatic metabolic homeostasis in mice, *Cell Death Dis.* 13 (2022) 279, <https://doi.org/10.1038/s41419-022-04725-9>.
- [51] M. Eckertova, M. Ondrejčáková, K. Krskova, S. Zorad, D. Jezova, Subchronic treatment of rats with oxytocin results in improved adipocyte differentiation and increased gene expression of factors involved in adipogenesis, *Br. J. Pharmacol.* 162 (2011) 452–463, <https://doi.org/10.1111/j.1476-5381.2010.01037.x>.
- [52] A. Romano, G. Provensi, Therapeutic potential of targeting the oxytocinergic system, *Int. J. Mol. Sci.* 23 (2022) 13295, <https://doi.org/10.3390/ijms232113295>.
- [53] L. Li, P. Li, J. Guo, Y. Wu, Q. Zeng, N. Li, X. Huang, Y. He, W. Ai, W. Sun, T. Liu, D. Xiong, L. Xiao, Y. Sun, Q. Zhou, H. Kuang, Z. Wang, C. Jiang, Up-regulation of oxytocin receptors on peripheral sensory neurons mediates analgesia in chemotherapy-induced neuropathic pain, *Br. J. Pharmacol.* 180 (2023) 1730–1747, <https://doi.org/10.1111/bph.16042>.
- [54] H.H. Burris, L.K. White, R. Waller, B.H. Chaiyachati, Oxytocin receptor epigenetics: from biomarker to potential therapeutic target, *Pediatr. Res.* (2024), <https://doi.org/10.1038/s41390-024-03686-3>.
- [55] R.E. Soccio, E.R. Chen, S.R. Rajapurkar, P. Safabakhsh, J.M. Marinis, J.R. Dispirito, M.J. Emmett, E.R. Briggs, B. Fang, L.J. Everett, H.-W. Lim, K.-J. Won, D.J. Steger, Y. Wu, M. Civelek, B.F. Voight, M.A. Lazar, Genetic variation determines PPAR $\gamma$  function and anti-diabetic drug response in vivo, *Cell* 162 (2015) 33–44, <https://doi.org/10.1016/j.cell.2015.06.025>.
- [56] S.N. Shapira, H.-W. Lim, S. Rajakumari, A.P. Sakers, J. Ishibashi, M.J. Harms, K.-J. Won, P. Seale, EBF2 transcriptionally regulates brown adipogenesis via the histone reader DPF3 and the BAF chromatin remodeling complex, *Genes Dev.* 31 (2017) 660–673, <https://doi.org/10.1101/gad.294405.116>.